

A unified approach to motion of grain boundaries, relative tangential translation along grain boundaries, and grain rotation

John W. Cahn^{*}, Jean E. Taylor

MSEL, NIST, Gaithersburg, MD and CIMS, NYU, New York, USA

Received 8 January 2004; accepted 18 February 2004

Abstract

We postulate that almost any motion of an interface between two crystals can produce a coupled tangential motion of the two crystals relative to each other which is proportional to the normal motion of the interface. Such translations can produce grain rotations; the special case of the rotations of shrinking included circular cylindrical grains which increase misorientation, as seen in the molecular dynamics simulations, is reinterpreted with this postulate. When this postulate is added to other principles of interface motion, several phenomena associated with grain boundary mechanics and motion are unified into a single theoretical formulation: normal motion of a grain boundary resulting from a shear stress applied tangential to it which results in tangential motion and its converse, tangential motion resulting from coupling to normal motion; rigid sliding of one grain with respect to the other along a “greased” boundary; grain rotation due to tangential motion along curved grain boundaries, produced by either by sliding or by coupling to the normal motion. When the motion is driven by the reduction in the total surface free energy $\int \gamma da$, if the grain rotation is due to sliding alone, then γ itself (the surface free energy per unit area) is reduced; if it is due to coupled motion, then increases in γ can occur if there is a large enough decrease in area that $\int \gamma da$ is decreased.

We explore the predictions for rotations of circular cylindrical grains moving to reduce total surface free energy. Among the surprising results is that certain combinations of coupling and surface free energy functions can result in increases rather than decreases in radii; these conditions, if achievable, can only occur far from small tilt misorientations. We also show that sliding alone must lead to misorientations with minimum γ – or no misorientation – before the crystal shrinks to zero radius. For coupling alone, limiting misorientations (which need not, and often do not, coincide with minima in γ) are never reached for non-zero radii. A more thorough exploration of sliding and coupling, including application to non-circular crystals and a variational model, is being published elsewhere. © 2004 Acta Materialia Inc. Published by Elsevier Ltd. All rights reserved.

Keywords: Grain boundary motion; Sliding; Shear; Grain rotation

1. Introduction

Two descriptions of tangential translations of one crystal relative to the other along a grain boundary have been proposed [1]. In one description, there is a *coupling* between the relative tangential translation of the crystals and the motion of the interface. When the interface is moving (with one crystal growing into the other), the

relative translation is distributed as a simple shear in the region traversed by the moving interface. Our paraphrased definition of simple shear is: every plane which is parallel “to the interface” moves itself in the direction of an axis “in the plane of the interface” through a distance proportional to the distance of the plane from the plane of the original interface [2,3].

In the other description the tangential translation along the grain boundary is not coupled to motion of the boundary. There is a rigid body translation, which we will call *sliding*, of one crystal relative to the other, as if the interface were “greased.” In this definition,

^{*} Corresponding author. Fax: +1-301-975-4553.
E-mail address: john.cahn@nist.gov (J.W. Cahn).

sliding occurs independently of other processes, and responds to a separate set of driving forces (which do not directly drive grain boundary motion, although some can drive other processes as well). The concepts of sliding and coupling for planar interfaces with an applied stress are illustrated in Fig. 1.

In Sutton and Balluffi [1], coupling is discussed in Sections 9.2.1.1 and 9.2.1.2, especially for the planar case for small tilt misorientations, while sliding is discussed separately in Section 12.8.1 for high angle grain boundaries. There is a comment “At some point, the mode of the bicrystal response should therefore switch.” No evidence of switching was found in the simulations of [4]. Twinning and martensite transformations are well known examples that coupling can persist to high angle grain boundaries. We cannot find any compelling evidence that coupling switches to sliding at high angles of misorientation.

Therefore in this paper, we postulate that switching does not occur and that coupling persists to all angles

(being absent only by reasons of symmetry and at certain angles where the coupling coefficient, β , defined below, changes sign) and explore some of its consequences. If true, almost any grain boundary can be moved by a stress through coupling, and the motion of almost any grain boundary will produce a relative tangential translation of the two grains.

Grain rotation, the relative rotation of the axes of two crystals, along a curved grain boundary also produces relative tangential displacement, and conversely, a relative tangential translation along a curved grain boundary would result in grain rotation. When there is coupling, motion of a circular cylindrical grain boundary produces rotation without requiring or developing any elastic stresses. This is illustrated in Fig. 2, which also shows how for small values of the misorientation θ between the grains, consideration of dislocations leads to a rotation to a higher misorientation. We propose that coupling, rather than sliding, may be a primary cause of grain rotation of non-circular grains as well

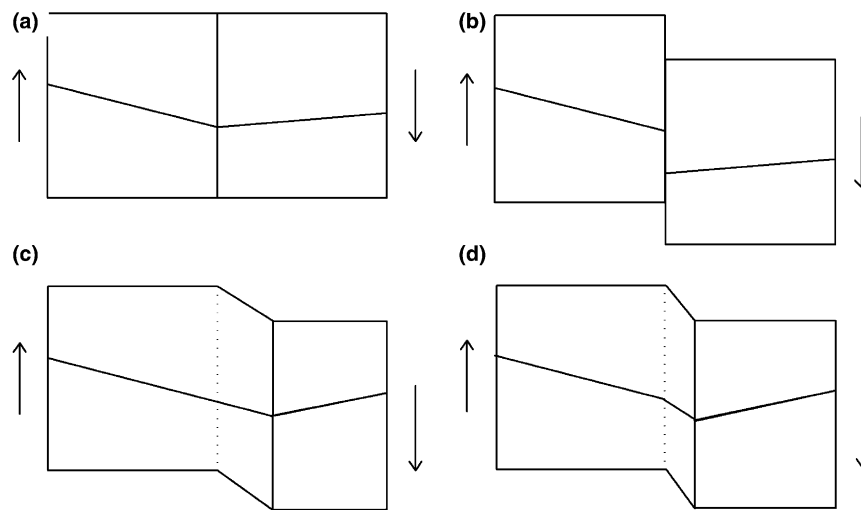


Fig. 1. Tangential motion of crystals along planar grain boundary typically occurs in response to an applied stress σ . Elastic distortions are small and not depicted. (a) Original bicrystal, showing grain boundary and the trace of a plane in each crystal. The positions of atoms along this trace is followed in the other parts of this figure. (b) Sliding without interface motion (greased boundary). (c) Coupling of relative tangential translation of crystals with interface normal motion without sliding; direction of interface normal motion determined by the coupling. Seen by Li et al. [6] and predicted in this paper to occur quite generally. (d) Coupling and sliding.

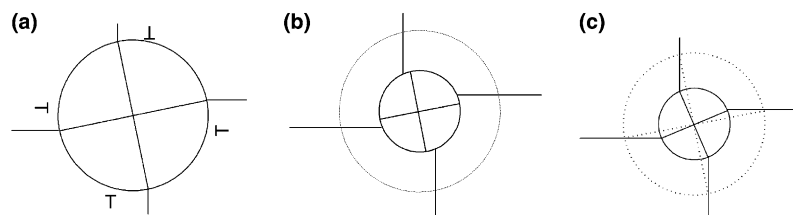


Fig. 2. When one of the crystals is a circular cylinder with radius r , included in the other and misoriented by α by a small rotation about the cylinder axis, tangential motion changes the rotation angle. Traces of two orthogonal crystal planes are shown, each crossing the entire cross-section and revealing edge dislocations, whose orientations are represented by \perp . (a) Original bicrystal. (b) Sliding alone, without normal motion, to decrease γ . Note that there is no dislocation mechanism for sliding regardless of whether the grain boundary moves. (c) Continuity of crossing planes must lead to an increase in misorientation as the included grain shrinks. This coupling of rotation driven by normal interface motion can also be understood through dislocation conservation. Although θ and γ increase when r decreases, $2\pi r\gamma$ decreases.

[5], and suggest that grain rotation during grain growth be reexamined and understood in terms of tangential translations and its two descriptions. We examine other consequences of coupling and sliding for grain boundaries and provide a single formulation for these various processes when effects of triple lines can be ignored.

Thermodynamic considerations can turn some observations of grain rotation into unambiguous evidence that grain rotation is coupled to grain boundary motion. In particular, in some of the recent isothermal simulations on cylindrical grains entirely included within matrix grains [4] gave rise to spontaneous grain rotations which increased θ , and thus, for a range of angles, γ , the surface free energy per unit area, as well. Thermodynamics specifies that the total free energy cannot increase in spontaneous isothermal processes. In these simulations the entire excess free energy (over that of a single crystal with the same number of atoms) is due to the grain boundaries and thus given by $\int \gamma da$, rather than just γ . For $\int \gamma da$ to decrease while γ increases, there must be a coupling to the motion of the curved grain boundary to produce a large enough decrease in grain boundary area.

When the misorientation between the grains is small, the observed rotation in [4] to higher tilt angle θ and thus to increasing γ can be explained as a simple shear produced by the conserved motion of the dislocations that comprise the grain boundaries. In the geometry of the simulation by Srinivasan and Cahn [4], dislocations are conserved because pairs of dislocations that could react and annihilate are diametrically opposed and thus widely separated. Therefore the density of dislocations in the grain boundary increases as area is lost, leading to higher θ . Since the rotation to higher misorientation was found to persist so smoothly to larger tilt misorientations, Srinivasan and Cahn surmised that the same phenomenon persists to all tilt misorientations, going through zero only where the shear changes sign. The final shrinkage of the grain was found to occur by amorphization.

A classic experimental example of what we believe to be coupling is in a paper by Li et al. [6], who found that approximately planar grain boundaries moved in their normal directions when a shear stress was applied along the grain boundary. It is easy to infer that the action of these shear stresses depended on a coupled relative displacement in the direction of the applied shear stress of one grain with respect to the other when the grain boundary moved. Conversely, we infer that normal motion of such a grain boundary, whether or not caused by an applied stress, would produce a coupled transverse displacement of one grain relative to the other. Although this normal motion requires coupling to the transverse motion, this is a case where the transverse motion could be supplemented (in the same or a different direction) by sliding. Any formulation must consider both.

Since in these experiments of Li et al. the misorientation between the grains was small, the authors inferred that the grain boundaries could be described as arrays of dislocations. Then the applied stress acted on these dislocations and caused their collective motion, being thus seen as moving grain boundaries. Elements in the traversed zone sheared and rotated from one crystal orientation to the other, while elements of the crystals away from the sheared zone experienced a rigid translation. Similar experiments have been done more recently with large misorientations [7], with the same observation that the grain boundary moved when a shear stress was applied.

Recently there have been many observations of grains rotating when grain boundaries move, both in experiments on grain growth grain [8] and in simulations on polycrystals [9–11]. The commonly accepted postulate is that the rotation of each grain is uncoupled to all grain boundary motions, including those leading to grain growth. The rotation of each of the grain is assumed driven by the reduction of $\int_{\text{each grain}} \gamma da$ for just the grain boundaries of that grain when its crystal axes are rotated without motion of its grain boundaries. Because these conditions on each of the grains have to apply simultaneously to all of the grains, they are difficult to substantiate (and to apply) for the usual grain growth experiments in polycrystals, where each grain has many neighbors and any rotation can cause the γ of some of its grain boundaries to increase (as long as the rotation will decrease the γ of the others more). Without coupling the standard capillary driving force on the grain boundary leads to motion by curvature to reduce area. The rotation is presumably by tangential sliding along the curved grain boundary, ignoring the obvious grain boundary motion required for the shape accommodation that is often needed. For the included bicrystal results, the uncoupled rotation postulate fails to permit γ to increase, and thus it is demonstrably invalid.

Bicrystal experiments [6,7] and simulations [4,9], where a grain has only one neighbor, have potentially less ambiguity. We first consider special cases in which the grain boundary between the two crystals does not terminate at a fluid phase or vacuum. A grain boundary along an infinite plane is one example; so are grains entirely included in a matrix grain. Certain geometries simplify the problem further. The tangential motion is constant along a planar grain boundary and for the circular cylinders studied by Srinivasan and Cahn [4] in which the rotation is along the cylinder axis. Then tangential motion can be accommodated without requiring mass transfer, and also for axial rotation of any included grain shape with cylindrical symmetry. When the included grain shape deviates from this symmetry, mass transfer must accompany grain rotation. This will be considered in a subsequent paper, using a variational formulation of shape accommodation by grain boundary diffusion [5].

Several complications are introduced into the bicrystal experiments [12,13] when a nearly planar crystal–crystal grain boundary terminates at a crystal–crystal–fluid triple junction line (at the “neck”). This situation is not addressed in this paper, but to illustrate the need to incorporate it in future work we summarize here what is known. It has been analyzed theoretically for nearly planar small angle dislocation grain boundaries [14,15]. For such small angle dislocation grain boundaries, the triple junction line plays two important roles: its thermal groove can pin the grain boundary (at the “neck”), greatly reducing curvature and normal motion, and it attracts and annihilates grain boundary dislocations, reducing θ . Since there is little area change, and indeed the neck may be growing in area, this produces the required reduction in γ . In these bicrystal experiments the relative motion is tangential only if the rotation axis is along the grain boundary normal (twisting); relative motion is along the normal if the rotation axis is in the plane (tilting). Both tilting and twisting occur if the axis is at a general angle. In any case the relative motion is not constant, but proportional to distance along the grain boundary from the rotation axis. For small angle grain boundaries, a model [14] based on climb or glide of grain boundary dislocations in response to the repulsion between them and their attraction to the contact line leads to a rotation rate proportional to $-\theta$ and not to $d\gamma/d\theta \approx \log \theta$; this model is confirmed by experiment [13]. In addition the rate of rotation is predicted to vary with the reciprocal of the length L (actually as $-(L \log L)^{-1}$) across the grain boundary between the triple junctions [14]. Thus triple line junctions between three crystals are likely to be important for rotation during grain growth in polycrystalline specimens and in geometric shape accommodation. A simulation to confirm this has been done [16]. Triple junctions are likely to be important in grain boundary motion and grain rotation in small-grained polycrystals, but their effects may become negligible when the extent of the grain boundary is large.

2. The model

We postulate that coupling comes from the biased diffusive atomic motions in the low symmetry environment of most grain boundaries which lead not only to a normal component to grain boundary motion, but also to a relative tangential one, which can occur in the absence of applied stress. Even when the atomic motions are diffusive and coupling has a statistical basis, we postulate a purely geometrical formulation, which need not be rational and crystallographic.

In a two dimensional description let \mathbf{n} be the normal direction of the interface, and \mathbf{t} the tangential direction chosen to be rotated clockwise from \mathbf{n} by 90° . Let $v_{\mathbf{n}}$ be the normal growth velocity, positive if in the direction \mathbf{n} , and v_{\parallel} be the rate of relative tangential translation of

the crystal into which \mathbf{n} points, positive if in the direction \mathbf{t} . For the combined effects of coupling and sliding,

$$v_{\parallel} = S\sigma + \beta v_{\mathbf{n}}. \quad (1)$$

Here β is the coupling constant, as without sliding equation (1) becomes $v_{\parallel} = \beta v_{\mathbf{n}}$, and S is the sliding coefficient in response to σ , the \mathbf{t} component of the applied stress; without coupling, $v_{\parallel} = S\sigma$.¹ The assumption of linear responses is not essential to anything we develop here. We postulate that β is a function of the misorientation θ between the crystals but not of the curvature, and that neither it nor S dependent on \mathbf{n} . We expect β to be continuous, except for θ at which there is a phase transition of the interface.

Since a tangential translation along a curved grain boundary produces a change in misorientation, the change in γ with misorientation can be a driving force for grain rotation, either with coupling or sliding. This is investigated for circular cylindrical embedded crystals below.

Because the experiment of Li et al. showed that a tangential stress σ produced a v_{\parallel} which could result from coupling alone or a combination of coupling and sliding, a challenge is to disentangle their effects. If under shear stress one sees in an experiment $v_{\mathbf{n}} = 0$ and $v_{\parallel} \neq 0$, then one has pure rigid sliding. If under some other driving force one sees $v_{\mathbf{n}} \neq 0$ and $v_{\parallel} = 0$, then $\beta = 0$ and $S = 0$ (one need not worry about the case where there is sufficient sliding to exactly balance the coupling, because any of a number of changes in experimental parameters will destroy the balance). When there is both normal and tangential motion, one needs to do additional experiments to determine β and S individually rather than in combination. Sometimes this can be with an analysis of the specifics of the atomic motions, which for small angle dislocation motion permit determinations of both β and S (see below). Or, for example, one might increase temperature which is expected to increase S greatly with little effect on β . Or one might do experiments in which there is a driving force for normal motion without a stress tangential to the grain boundary. Differences in the volume free energy f_V provide examples of such driving forces; for example, a homogeneous magnetic field produces differences in the energy of variously oriented diamagnetic grains, and thus creates a driving force for normal motion [17–19]. Elastic loading of the bicrystal with anisotropic crystals creates differing strains along \mathbf{n} alone, and provides a driving force for the

¹ When considering the full 3-dimensional problem, one has to recognize that v_{\parallel} is a vector in the interface plane, that $v_{\mathbf{n}}$ is along the normal, and that β and σ are tensors in the interface plane. If both crystals have mirror planes which are parallel and which contain \mathbf{n} , then β will not have a component out of that common mirror plane and can be treated as a scalar, as in Eq. (1). Furthermore if the bicrystal has a two-fold axis in the interface plane or a common even-fold axis along \mathbf{n} , β will be zero perpendicular to those axes.

growth of the grain with the larger compliance which is an even function of the applied stress. We therefore include forces capable of inducing normal motion of grain boundaries in our formulations. In the presence of such fields f_V might depend on the orientation of each of the grains. In Section 4 the orientation of one grain is held fixed, and thus f_V becomes a function of θ alone. Any dependence of f_V on θ creates issues discussed in the notes added in proof.

One further part of the model developed here is the assumption that v_n is linear in the driving force, via a mobility M which may depend on many variables such as misorientation θ and temperature, composition, etc. That is, when the normal velocity is v_n , the rate of change of free energy plus work done (per unit area of a at interface) is $-(f_V v_n + \sigma v_{||})$ which with Eq. (1) becomes $-(f_V v_n + \sigma(S\sigma + \beta v_n))$. Therefore, for a interface,

$$v_n = M(f_V + \sigma\beta) \tag{2}$$

and so

$$v_{||} = S\sigma + \beta M(f_V + \sigma\beta). \tag{3}$$

(Again, this linearity assumption on the mobility could be replaced by a different kinetic assumption.) Thus when the normal motion is due only to shear stress σ (i.e., $f_V = 0$),

$$v_n = M\beta\sigma, \quad v_{||} = (S + M\beta^2)\sigma. \tag{4}$$

When $\sigma = 0$,

$$v_n = Mf_V, \quad v_{||} = \beta Mf_V. \tag{5}$$

When normal motion is due only to capillarity with β and σ both zero, and when γ is independent of \mathbf{n} and the interface is cylindrical with radius r (with normal \mathbf{n} pointing into the cylindrical crystal), then we have the usual $v_n = M\gamma/r$ and $v_{||} = 0$. For the formulation of these slow velocities, originating from diffusive processes, momentum is not a factor.

For circular cylindrical crystals and a surface free energy γ which is independent of the normal directions of the interface, capillarity is combined with coupling, sliding, and body forces in Section 4. A more thorough exploration, including application to non-circular crystals, is being published elsewhere [5]. It relies on a novel variational formulation of grain boundary motion due to surface diffusion in the presence of normal grain boundary motion.

3. Special cases and the general the coupling conjecture

3.1. Dislocation-based analysis for tilt boundaries with small misorientations

We regard crystal B as having its lattice rotated from the other crystal A in a counter-clockwise direction

about a common axis by angle θ . If the normal \mathbf{n} to the plane of the boundary is perpendicular to the common axis a tilt boundary is created; if the normal is along the common axis a twist boundary is created. The unit normal \mathbf{n} of the interface is the exterior normal to A and points into crystal B , and thus the normal velocity v_n will be that seen from A .

With a low density of dislocations, the lattices of the two crystals change continuously across the interface, except for the dislocations. Therefore if the misorientation θ is small in magnitude in a symmetric tilt boundary, the motion of the interface is by the dislocations gliding along \mathbf{n} . Then just by geometry this is an example of coupling with

$$\begin{aligned} v_{||} &= 2 \tan(\theta/2) v_n \approx \theta v_n, \\ \beta &= 2 \tan(\theta/2) \approx \theta. \end{aligned} \tag{6}$$

For the pure symmetric tilt boundary there are no dislocations which can glide in the plane of the boundary. Hence there is no dislocation mechanism for sliding, and $S \equiv 0$ unless σ approaches the theoretical strength of perfect crystals. (Some rigid sliding together with coupling might occur, due e.g. to a wetting or premelting layer on the grain boundary mediated by impurities or high temperatures.) Note that β would have been zero if the σ had been applied along the dislocation lines, i.e. perpendicular to the two-fold axis in a symmetric tilt boundary. The screw dislocations in a twist boundary can glide; hence S is positive, while symmetry dictates that $\beta = 0$ if the rotation is about an even-fold axis. An arbitrary mixed boundary with tilt and symmetric twist components should have both S and β non-zero.

Consider such a grain boundary with normal $\mathbf{n} = (1, 0, 0)$, made from one type of dislocation, with Burgers vector (sign chosen as defined by [20], p. 45) $\mathbf{b} = b(1, 0, 0)$. The misorientation is then $\theta = \rho b$, where ρ is the density of the dislocations; observe that $b > 0$ if and only if $\theta > 0$. The Peach–Koehler formula (e.g. [20], p. 355) gives the force on a unit length of dislocation line with direction $l = (0, 0, 1)$ and Burgers vector \mathbf{b} due to stress tensor σ :

$$f_m = -\epsilon_{mjl} \ell_n \sigma_{ij} b_i. \tag{7}$$

Here $\epsilon_{ijk} = 1$ if $ijk = 123$ or 231 or 312 , -1 if $ijk = 321$ or 132 or 213 , and 0 otherwise. With

$$\sigma = \begin{pmatrix} 0 & \sigma & 0 \\ \sigma & 0 & 0 \\ 0 & 0 & 0 \end{pmatrix}, \tag{8}$$

the glide force (f_m resolved in the plane containing \mathbf{b} and ℓ_n) is,

$$f_1 = -\epsilon_{132} \sigma_{12} b_1 = -\sigma b, \tag{9}$$

while the climb force (f_m out of this plane) is zero,

$$f_2 = -\epsilon_{231} \sigma_{21} b_2 = 0. \tag{10}$$

Assuming that v_n results from motion of the individual dislocations, whose velocity is assumed herein to be linear in the glide force, we obtain

$$v_n = M_b \mathbf{f} \cdot \mathbf{n} = M_b b \sigma. \quad (11)$$

For an interface with normal \mathbf{n} composed of several different types of dislocations,

$$\theta_n = \sum_i \rho_i \mathbf{b}_i, \quad (12)$$

where the subscript i denotes dislocations of the i th type and ρ_i is their density. While all the dislocations must move together to keep a at interface with normal \mathbf{n} , there are complications. For example some dislocations are more mobile than others, and different types of dislocations will cross and react. Considering only the mobility differences, via penalty terms in a variational approach detailed in the companion paper [5], one obtains

$$v_n \mathbf{n} = \frac{1}{\sum_i \rho_i / M_{b_i}} \left(\sum_i \rho_i \mathbf{b}_i \right) \sigma. \quad (13)$$

If we compare this with the general statement $v_n \mathbf{n} = M \beta \sigma \mathbf{n}$, and use $\beta = \theta$, we see that for a single species of dislocation

$$M = M_b / \rho = M_b b / \theta. \quad (14)$$

More generally, $M = \frac{1}{\sum_i \rho_i / M_{b_i}}$, a harmonic average of the individual dislocation mobilities M_{b_i} , weighted by their densities.

3.2. Symmetric twist boundaries

A similar calculation for a symmetric twist boundary shows it is composed of screw dislocations which can glide in the plane of the boundary in response to σ , giving rigid sliding and thus $S \neq 0$. With an appropriate stress these same screw dislocation can also glide along \mathbf{n} moving the boundary with them. But there exist bicrystals with special symmetries which make any positive and negative motion equivalent and ensure that β is zero. For example, there is at least one two-fold axis of the bicrystal in the plane of any symmetric twist boundary; if a tangential shear stress is applied normal to that, $\beta = 0$ by symmetry.

The symmetric tilt and twist boundaries are two examples for which one can choose conditions were either S or β must be zero by symmetry. We have also given examples where there are dislocation mechanisms to make S or β non-zero.

3.3. Mechanical twinning

Twinned bicrystals are variously defined² by orientation relationships among the two grains, and a twin

² There seem to be many definitions of what precisely constitutes a twinned bicrystal.

boundary is the grain boundary between them. Some twin boundaries can be moved by an applied stress [3]. This coupled motion under stress is called mechanical twinning, and provides well-understood examples of high angle grain boundaries for which $\beta \neq 0$ and related to the twinning shear. Those β are easily measured and related to the bicrystal geometry on an atomic level. Thus twinning provides data about β , especially useful if we assume β is a continuous function of β .

Twin boundaries that cannot be moved by mechanical stress reveal zeroes of β . Some of these zeroes occur by reasons of symmetry and can be easily found, but there are other interesting zeroes. Friedel [21,22] made the existence of a twin lattice, now called coincidence site lattice (CSL), a defining characteristic of twins, and would have considered $\Sigma 5$ grain boundaries in fcc as twin boundaries. Since β was found to be zero in simulations [4] for $\Sigma 5$ grain boundaries, these Friedel twins are not mechanical twins. They would not be considered twins in some other definitions, even in those that do not depend on mechanical coupling.

3.4. A conjecture that coupling occurs almost always

There are many mechanisms for expecting coupling at higher misorientations when dislocation models are no longer applicable. Growth of one grain into another can be thought of as the rotation of small groups of atoms from one lattice to the other [23], and unless there is special symmetry those rotations are biased by the lack of symmetry and add up to a net tug. Consider instead applying the structural unit model in two steps to a moving grain boundary. As the boundary approaches a portion of one periodic crystal opens up and distorts to form a structural unit; when the boundary passes the structural unit collapses to form a portion of the other grain. Unless there are special symmetries there is a component of the mean translation along the boundary which carries the respective crystals along to provide the translation [5].

We conjecture that β can be expected almost always to be non-zero. The exceptions are when there are special symmetry conditions or where β changes sign.

4. Rotation of circular cylindrical grains

Assume there is a cylindrical crystal B with a circular cross-section radius $r(t)$ and misorientation $\theta(t)$ entirely inside another crystal A . We work entirely in two dimensions (the cross-section of the cylinder) but continue to use the language (surface area, etc.) of three dimensions. The orientation of the outer crystal A is held fixed. From the point of view of A (so that \mathbf{n} points into B and the tangent \mathbf{t} points counterclockwise), a rotation of B to change the angle by $d\theta$ amounts to a relative displace-

ment in the direction of \mathbf{t} along the grain boundary and a radial change dr amounts to normal motion:

$$r(t)d\theta = v_{\parallel}dt; \quad dr = -v_{\mathbf{n}}dt. \quad (15)$$

Grain boundary motion is driven by the rate of reduction of total free energy per unit cylinder height (composed of surface free energy plus a bulk free energy difference f_V per unit volume)

$$\frac{dF}{dt} = \frac{d}{dt}(2\pi r(t)\gamma(\theta(t)) + \pi r^2 f_V), \quad (16)$$

and the rate of work done, also per unit height, by an applied stress σ along the boundary in the direction \mathbf{t} ,

$$\frac{dW}{dt} = -2\pi r^2 \sigma \frac{d\theta}{dt}. \quad (17)$$

The sum of these is then

$$\frac{dF}{dt} + \frac{dW}{dt} = 2\pi r \left(\left(\frac{\gamma}{r} + f_V \right) \frac{dr}{dt} + \left(\frac{\gamma'}{r} - \sigma \right) r \frac{d\theta}{dt} \right), \quad (18)$$

which indicates that γ/r and $-\gamma'/r$ act effectively like additions, respectively, to f_V and the applied stress σ . Eq. (1) becomes

$$r \frac{d\theta}{dt} = -\beta \frac{dr}{dt} + S \left(\sigma - \frac{\gamma'}{r} \right). \quad (19)$$

Thus

$$\frac{dF}{dt} + \frac{dW}{dt} = 2\pi r \left(\left(\frac{\gamma}{r} + f_V - \beta \left(\frac{\gamma'}{r} - \sigma \right) \right) \frac{dr}{dt} - S \left(\frac{\gamma'}{r} - \sigma \right)^2 \right), \quad (20)$$

which together with assuming a linear response to the driving force, via a mobility M , become the main equations for the predicted behavior of circular cylinders

$$-v_{\mathbf{n}} = \frac{dr}{dt} = -M \left(f_V + \frac{\gamma - \beta\gamma'}{r} + \beta\sigma \right), \quad (21)$$

$$\begin{aligned} -v_{\parallel} &= r \frac{d\theta}{dt} \\ &= \beta M \left(f_V + \frac{\gamma - \beta\gamma'}{r} + \beta\sigma \right) - S \left(\frac{\gamma'}{r} - \sigma \right). \end{aligned} \quad (22)$$

Observe that these equations approach those for a planar interface when r is large, as they should. Time is eliminated by dividing Eq. (21) into (22) (if $dr/dt \neq 0$), showing that a direct relation between changes in θ and r can be expressed as a sum of the coupling coefficient β and a sliding term.

$$\frac{d\theta}{d \ln r} = \beta + \frac{(\gamma'/r + \sigma)}{M[f_V + (\gamma - \beta\gamma')/r + \beta\sigma]} S. \quad (23)$$

We now discuss various conclusions obtained from Eqs. (21) and (22). Because parameters such as M , S , γ , and even f_V can depend on θ , these equations usually have to be solved simultaneously.

4.1. No coupling and no sliding ($\beta=0$, $S(\sigma - \gamma'/r) = 0$)

We begin with the case where there is neither coupling nor sliding, and, consequently according to Eq. (22), no rotation; θ is constant. Then Eq. (21) reduces to motion by well-known driving forces, $f_V + \gamma/r$,

$$-v_{\mathbf{n}} = \frac{dr}{dt} = -M \left(f_V + \frac{\gamma}{r} \right). \quad (24)$$

For example, if $f_V = 0$ then motion is by curvature and we can integrate and solve this equation for $r(t) = \sqrt{r_0^2 - 2M\gamma t}$, where r_0 is the initial r . The cylinder shrinks to $r = 0$ at $t_{r=0} = r_0^2/2M\gamma$.

4.2. Sliding only ($\beta=0$ and $S(\sigma - \gamma'/r) \neq 0$)

Whenever $\beta=0$, Eq. (24) holds for dr/dt , while Eq. (22) becomes

$$r d\theta/dt = -S((\gamma'/r) - \sigma). \quad (25)$$

The direction of rotation is determined by the sign of $(\gamma'/r) - \sigma$. Since the grain is circular, σ exerts a torque. When the magnitude of σ is sufficient ($|\sigma| > |\gamma'/r|$), then σ overwhelms the capillary driving force and determines the direction of rotation.

If $\sigma=0$, Eq. (22) becomes $d\theta/dt = -S\gamma'/r^2$. Grain rotation is to decrease γ . For small $|\theta|$, the result of Read and Shockley [24] gives

$$\gamma(\theta) = a_1|\theta| + a_2|\theta| \ln(1/|\theta|). \quad (26)$$

Then $\gamma' \rightarrow \infty$ as $\theta \downarrow 0$, and rotation by sliding is towards coincidence of crystal axes with ever increasing rate, assuming that S does not go to zero too fast and that an applied f_V does not push r to grow fast.

If we assume that both $f_V = 0$ and $\sigma = 0$, Eq. (21) becomes motion by curvature, $dr/dt = -M\gamma/r$, but with M and γ changing with θ , while Eq. (23) becomes

$$\frac{d\theta}{d \ln r} = \frac{S\gamma'}{M\gamma}. \quad (27)$$

When $\gamma(\theta)$, as well as $M(\theta)$ and $S(\theta)$, are known this equation can be integrated to give how θ depends on r . Then γ , as well as M and S , can be given as functions of r and (21) integrated to obtain $r(t)$.

Consider a circular grain with small tilt angle. In the limit of small θ , the Read–Shockley result [24] for γ gives $\gamma'/\gamma \approx 1/\theta$. Integration of (27), with r_0 and $\theta(r_0)$ as the initial r and θ . If we assume S and M are constant, this results in

$$\theta(r_0)^2 - \theta(r)^2 = (2S/M) \ln[r/r_0], \quad (28)$$

and we see that the two grains merge by (sliding) rotation to reach $\theta=0$ when $r_{\theta=0}/r_0 = \exp[-M\theta(r_0)^2/2S]$, i.e. before the cylindrical grain has shrunk to $r=0$. This is the situation of the phase-field model assumed by [11]. On the other hand, if we assume $M = M_b b/\theta$ (14) and

$S = S^*\theta^2$ (arbitrary for purposes of illustration, since S should be close to zero for small $|\theta|$), then instead we get $-1/\theta(r) + 1/\theta(r_0) = (2S^*/M_b b) \ln[r/r_0]$. (29)

Now the radius goes to zero as θ goes to zero. Therefore whether or not there is coincidence before the inner grain shrinks to zero radius depends on the assumptions about M and S – and on whether r_0 is small enough that these approximations are appropriate.

Next consider a grain with misorientation θ close enough to a local minimum γ_m in γ at $\theta = \theta_m$, and assume (more reasonably here) that S and M are constant; approximate γ by $\gamma(\theta_m) + a_n|\theta - \theta_m|^n$ for some $n > 0$. Then $\gamma'/\gamma \approx na_n|\theta - \theta_m|^{n-1}/\gamma_m$. When $n \neq 1$ or 2 , integration of (27) yields

$$|\theta - \theta_m|^{2-n} - |\theta(r_0) - \theta_m|^{2-n} = \frac{na_n S}{(2-n)\gamma_m} \ln \frac{r}{r_0}.$$

For $n < 2$ (and $n \neq 1$) we see that r approaches a non-zero limit as θ approaches θ_m ; the opposite is true for $n > 2$. The special case of $n = 1$ is not really a special case, as its integration also says r approaches a non-zero limit. For the dividing case of $n = 2$, integration of (27) leads to

$$\ln \frac{\theta - \theta_m}{\theta(r_0) - \theta_m} = \frac{2a_2}{M\gamma_m} \ln \frac{r}{r_0},$$

and grains reach θ_m only in the limit of $r = 0$. For integration of (21), setting γ to γ_m is a good approximation, and $r(t) \approx \sqrt{r_0^2 - 2M\gamma_m t}$.

4.3. Coupling only ($S = 0$ and $\beta \neq 0$)

When $S = 0$, Eq. (21) is not affected, while Eqs. (22) and (23) become

$$-v_{||} = r \frac{d\theta}{dt} = -\beta M \left(f_v + \frac{\gamma - \beta\gamma'}{r} + \beta\sigma \right), \quad (30)$$

$$\frac{d\theta}{d \ln r} = -\beta. \quad (31)$$

Comparing Eqs. (31) and (23) shows that the absence of a radius dependence provides a test for the absence of sliding.

The second equation should provide the basis for a convenient method for determining β as a function of θ from the simulations: when there is no sliding, all $\log_{10} r$ versus θ plots of results should superimpose on a master curve after shifting the graphs vertically to account for differences in the integration constants due to differences in the initial r . This is illustrated in Fig. 3 and discussed below.

Although the equations are constructed from a thermodynamic formulation and guaranteed to be consistent with thermodynamics, it is noteworthy that none of the driving force factors, not f_v , γ , not even σ and γ' , the main driving forces for rotation by sliding in

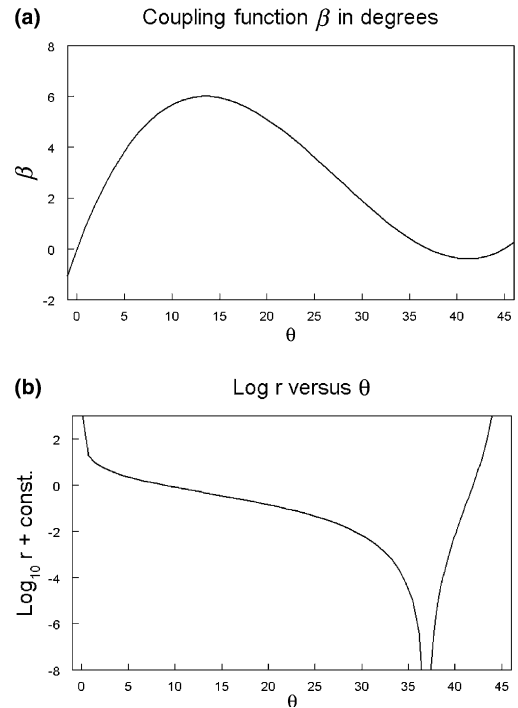


Fig. 3. (a) A sample coupling function β , Eq. (34), with $\theta_1 = 36.87^\circ$, and $\theta_2 = 45^\circ$, plotted against θ . (b) The corresponding master curve from the integration of Eq. (31), on a log-log plot. When there is no sliding, all $\log_{10}[r]$ versus θ plots of results for this β should superimpose after shifting the graphs vertically to account for differences in the initial conditions and thus differences in the integration constants c_1 and c_2 .

Eq. (25), appear in Eq. (31). It emphasizes that rotation due to coupling alone is purely geometric.

(i) From Eq. (30) or (31) we see that θ is constant when $\beta(\theta) = 0$. Therefore, when there is no sliding, the zeroes of β rather than the minima of γ are the candidates for constant θ .

An obvious zero of β is $\theta = 0$. For small angle tilt misorientations, Eq. (6) holds, and with $\sigma = 0$, θ can be substituted for β and Eq. (31) specializes to

$$\frac{d \ln |\theta|}{d \ln r} = -1,$$

which integrates to

$$r(t)\theta(t) = \text{constant} = r_0\theta(r_0), \quad (32)$$

a result consistent with dislocation conservation and with the simulation [16]. According to (32), the zero in θ at $\theta = 0$ occurs only at $r = \infty$; it is never reached in this coupling-only situation.

Suppose $\beta(\theta_i) = 0$ for some other θ_i . Then for θ near θ_i , let β be approximated by $\beta = \beta'(\theta_i)(\theta - \theta_i)$, where $\beta'(\theta_i) = (d\beta/d\theta)$ at $\theta = \theta_i$. Then, if $\beta'(\theta_i) < 0$, θ moves toward θ_i as the grain shrinks. If $\beta'(\theta_i) > 0$, the grain rotates away from θ_i as it shrinks. (This case includes the small angle tilt boundaries considered above.) Integrating Eq. (31) gives

$$\frac{\theta - \theta(r_0)}{(\theta(0) - \theta(r_0))} = \left(\frac{r}{r_0}\right)^{-\beta'(\theta_0)}, \quad (33)$$

which reveals that even when $\beta'(\theta_0) < 0$, θ approaches θ_i only in the limit as the grain radius shrinks to zero. This could not be seen in the simulations, because the grains always became amorphous [16] when r was about 5 atomic radii.

(ii) As stated above, for any given function β of θ , integrating Eq. (31) gives a master equation which relates r to θ . Let us assume for illustrative purposes that β can be approximated by a polynomial,

$$\beta = \theta(1 - \theta/\theta_1)(1 - \theta/\theta_2), \quad (34)$$

with $0 < \theta_1 < \theta_2$; this function has the proper behavior at small θ and has zeroes at θ_1, θ_2 . Integrating Eq. (31) gives

$$\log r = \log(\theta) + \frac{1}{\theta_2 - \theta_1} (-\theta_2 \log(\theta_1 - \theta) + \theta_1 \log(\theta_2 - \theta)) + c_1 \quad \text{for } 0 < \theta < \theta_1,$$

$$\log r = \log(\theta) + \frac{1}{\theta_2 - \theta_1} (-\theta_2 \log(\theta - \theta_1) + \theta_1 \log(\theta_2 - \theta)) + c_2 \quad \text{for } \theta_1 < \theta < \theta_2.$$

The integration constants are determined by inserting a known r and θ , say r_0 and $\theta(r_0)$.

For tilts about a common cube [001] axis in fcc, \mathbf{n} lies along the (001) common mirror plane. Then symmetry dictates that zeroes in a continuous (vector or scalar) β occur at every even-fold axis in the (001), i.e. at $\theta = n\pi/4$ for every integer n . The simulation [4] found another set of zeroes for $\Sigma 5$ at $\theta = 2 \tan^{-1}(1/3) = 0.6435^\circ$ or 36.87° , to be repeated by the 4mm symmetry of the (001) plane. At the high temperature of the simulation, no zeroes were found at $\Sigma 13$ and $\Sigma 17$. A polynomial β with three specific zeroes at $\theta = 0^\circ$, $\theta = \theta_1 = 36.87^\circ$, and $\theta_2 = 45^\circ$ is plotted against β in Fig. 3(a). Fig. 3(b) shows the corresponding master curve for this β . The ordinate is $\log_{10}[r]$. When there is no sliding, all $\log_{10}[r]$ versus θ plots of results should superimpose after shifting the graphs vertically to account for differences in the initial conditions and thus differences in the integration constants c_1 and c_2 .

This master curve illustrates that with decreasing r , grains rotate to approach the zero at $\Sigma 5$ only in the limit of $r = 0$, and rotate away from $\theta = 0^\circ$ and 45° . Since the change in θ per decade change in r of a typical simulation is small, many simulation runs with different starting θ would be needed to map out β .

(iii) From Eq. (21) we see that the inner grain grows rather than shrinks if $f_v + \frac{\gamma - \beta\gamma'}{r} - \beta\sigma < 0$. This can happen even if $\sigma = 0$ and $f_v = 0$ provided $\gamma - \beta\gamma' < 0$. No experiments have yet found a range of θ and functions β and for which this condition holds; in particular, it

is incompatible with small angle tilt boundaries. Still, if such a condition were to hold over some range of larger angles, this might give rise to opportunities to keep grain size fixed and small.

If the applied torque from the stress σ is non-zero, it will move the curved boundary by coupling in the same way as in the experiments of [6]. According to Eq. (21), a large enough stress, $\beta\sigma > f_v + (\gamma - \beta\gamma')/r$, will cause the grain to grow. By Eq. (30) or (31) rotation will reverse as well.

Consider conditions where the stress balances the other factors and $\beta\sigma = f_v + (\gamma - \beta\gamma')/r$. Both growth and rotation cease. For any fixed σ , we can solve for an r for which $dr/dt = 0$; because smaller cylinders shrink and larger ones grow, this r is unstable. When the crystals are prevented from rotating, $d\theta/dt = 0$; σ will take on the value in the above equation and the grain will not grow or shrink.

(iv) For small angle tilt boundaries all elements of Eqs. (30) and (31) are known. When f_v and σ are zero, the normal velocity is proportional to $1/r$, but with factor $M(\gamma - \beta\gamma')$ rather than $M\gamma$. We may use Eq. (26) to compute

$$\gamma - \beta\gamma' = \gamma - \theta\gamma' = a_2|\theta| > 0. \quad (35)$$

Using the expression (14) for M , the motion laws become

$$-v_n = \frac{dr}{dt} = -\frac{M_b b a_2}{r}, \quad (36)$$

together with the general coupling-only result $r\theta = \text{constant}$. The θ dependence of M in Eq. (14) cancels that in β . Integrating and solving for $r(t)$ yields $r(t) = \sqrt{r_0^2 - 2M_b|b|a_2t}$. This looks like the classical result $r(t) = \sqrt{r_0^2 - 2M\gamma t}$, but it will have a very different dependence on temperature.

The increase in θ occurs in spite of the fact that γ' is large and positive when θ is small and positive, because the integral γ , namely $2\pi r\theta(a_1 + a_2 \ln(1/\theta)) = 2\pi r_0\theta_0(a_1 + a_2(1/\theta))$, decreases in time in spite of the increase in $\gamma(\theta)$ itself.

4.4. Coupling and sliding

Finally, observe that the full equations (21)–(23) produce the many additional cases for which there is both coupling and sliding, including the many limiting conditions, detailed above, for which either sliding or coupling become large enough to overwhelm the other.

In many experiments we do not know whether coupling or sliding or both are occurring. Adding Eq. (21), multiplied by β to (22) we obtain

$$\beta \frac{dr}{dt} + r \frac{d\theta}{dt} = -S \left(\frac{\gamma'}{r} - \sigma \right). \quad (37)$$

The differences in the dependencies of the various terms on shrinkage and rotation rates, r and σ should enable the determination of β and S . The task is much simpler if β is known.

When there is both sliding and coupling, θ will tend to alternate zeroes of the RHS of Eq. (23), those with the positive sign of the θ coefficient of the RHS. Since there is an r dependence in the sliding term, these zeroes will change with time as the cylinder shrinks.

Consider the small θ case with $f_V=0$ and $\sigma=0$; dr/dt is negative and given by Eq. (36). The sign of $d\theta/dt$ depends on the ratio $\frac{S\gamma'}{M\theta(\gamma-\theta\gamma')}$. If it is larger than 1, θ will decrease. We have seen from Eq. (14) that $M\theta$ is approximately constant (equal to $M_b b$). If S were constant in the small θ limit, sliding would always overcome coupling for small enough θ (since $\frac{\gamma'}{\gamma-\theta\gamma'} \approx \frac{-\ln|\theta|}{\theta}$ gets large without bound as θ approaches zero) and θ would tend to zero. However, the absence of dislocations for sliding and the simulations imply that S tends to zero fast enough to make the ratio tend to zero, or at least limit its magnitude so that the grain rotates to increase θ and take the grain out of the small- θ range.

5. Discussion

Coupling and sliding are much discussed [1] as disparate basic concepts in the literature of relative tangential motion of two crystals at the interface between them. In Eq. (1) we combined these concepts into a single formulation, based on our belief that both can occur for any given interface, sliding in response to a shear stress and coupling due to the biased motion of atoms in the anisotropic environment of the moving interface. Sliding will be absent when symmetry or the absence of appropriate dislocation makes $S=0$. It will also be absent when there is no stress or if $\gamma'=0$ along a curved interface. Coupling can be absent at values of θ for which the coupling coefficient $\beta=0$; this usually occurs at special values of θ where a continuous β changes sign, often for symmetry reasons. Abrupt cessation of coupling can only come at first-order interfacial phase transitions, such as interfacial melting. We therefore postulated that almost any motion of an interface between two crystals can produce a coupled tangential motion of the two crystals, with or without an additional rigid sliding produced by an applied stress.

Through the purely geometric equation (15) we linked this tangential motion of planar interfaces to grain rotation. This concept relates the causes and mechanisms of grain rotation to every cause and mechanism for tangential motion. In Section 4 we illustrated some of the many consequences on rotation and shrinkage of circular cylindrical embedded crystals. In future work we intend to extend these to the causes and effects

of grain rotation on grain growth and during high-temperature mechanical processing.

Knowledge about the coupling constant β comes from simulations [4,9], experiments [6,7], mechanical twinning, and symmetry. For small angle tilt boundaries, dislocation theory results in Eq. (6) for $\beta(\theta)$. For twist boundaries, β is zero by symmetry. Symmetry is a useful tool for finding many other zeroes where β changes sign, but not all zeroes are dictated by symmetry. In the absence of interfacial phase transition, β is continuous, allowing e.g. use of Eq. (6) and the zeroes found in simulations and from symmetry to estimate and sketch out the $\beta(\theta)$ in Eq. (34) and Fig. 3(a).

Dislocation theory and symmetry provide some insight into the sliding parameter S . Because symmetric tilt boundaries do not contain any of the dislocations needed for sliding, $S=0$ for any θ . Moreover thermodynamics does not allow S to be negative.

Because of the continuity of β and S , there seems to be no reason to expect a switching from coupling only to sliding only at some misorientation angle θ . Our postulate is that they can occur together, even though, for some interfaces and under some circumstances, either coupling or sliding, or both, can be absent.

In Eqs. (2) and (3) we introduced kinetics through an interfacial mobility M and an extra term, a volume driving force f_V , to suggest experiments for the independent determination of the parameters. In Eqs. (21)–(23) these kinetics were extended to shrinkage (and growth) and rotation of embedded grains which are circular cylinders.

Since Eqs. (21)–(23) contain many parameters and terms, we explored in Sections 4.1–4.4 many simpler situations for such embedded grains in which one or more factors can be ignored, either as limiting cases, or eliminated through the design of experiment. The results show grain shrinkage by curvature, modified by f_V in Eq. (24) or simple dislocation dynamics in Eq. (36) or in Eq. (37) linked by coupling to rotation rate, as well as to γ' and σ . When sliding is dominant, the rotation rate given in Eq. (22) simplifies to that in Eq. (25), and demonstrates a dependence on σ , which acts as a torque, and is supplemented by a dependence on γ' . When coupling is dominant the rotation rate depends on quite different parameters given in Eq. (30).

Elimination of time leads to a simpler equation (23) which contains a coupling and a sliding term and which relates the changes in θ directly to changes in r . From this a set of simpler equations are derived, allowing rotation due to sliding and coupling alone to be examined. The contrast between Eqs. (27) and (31) is most revealing. With sliding alone (and $\sigma=0$), rotation is towards minima in γ , while with coupling alone the rotation is towards and away from alternate zeroes in β . Most dramatically, Eq. (32) shows that coupled shrinking moves θ to higher γ , away from the cusped minimum

in γ at $\theta=0$. This result is consistent with what was found in simulations [4] and with thermodynamics.

We have thus unified into a single theoretical formulation at least five disparate phenomena associated with grain boundary kinetics and mechanics. Three result from an applied shear stress along a planar grain boundary:

1. Sliding of one rigid grain with respect to the other tangentially along a stationary grain boundary.
2. Coupling of the normal motion of a grain boundary with tangential motion, resulting in a sheared zone in the region traversed by the grain boundary, and, as a special case.
3. Mechanical twinning. The other two apply to curved grain boundaries for which there can be grain boundary motion without the need of an applied shear stress; tangential motion produces rigid rotation of one grain relative to the other.
4. Sliding driven by a stress or by the reduction in γ , not coupled to the normal motion and thus independent of a reduction in area, and
5. Coupling of the tangential motion and thus grain rotation to the usual grain growth processes, driven by the reduction in the $\int \gamma dA$.

We believe a unified formulation is needed because the same physics is involved in all these phenomena. The underlying molecular processes are similar and thus the same kinetic coefficients are likely to occur. Each of the processes could occur locally in many different situations, but data obtained from one should be useable in each of the others. Tangential motion in grain growth is linked to grain rotation and mechanical twinning.

Similar-looking sheared zones in surface topography can result from tangential motion whenever there is boundary normal motion, whether coupling or sliding occurs. In the experiments of Li et al. [6], coupling is implicated as there was no normal component of the applied driving force and the interfaces were flat. However, in the classic work of Wheeler and Hanson on the surface topography during creep [25,26], which clearly revealed tangential motion along advancing grain boundaries, the grain boundaries could be advancing independent of the transverse motion for two reasons, because they were curved and there was deformation, which could have led to recrystallization. Thus either coupling or sliding or both could be occurring.

We suggested several strategies for disentangling the mechanisms, varying driving forces to separate σ from γ'/r , changing curvature and θ , varying the parameters S and β through dislocation types, and varying S and M with temperature and impurities. But the most dramatic difference occurs during the shrinkage of circular grains. With sliding, the grain reached an “equilibrium” with respect to θ , usually before it had shrunk to $r=0$,

while for coupling the direction of the rotation was not influenced by minima in γ , and in the case of small θ dramatically rotated away from a cusped minimum in γ . Even when the sign of the coupling constant β favored rotation towards a zero in β , the rotation reached that angle only in the limit of $r=0$. We also included forces due to volume free energy difference, such as those due to magnetic fields, which drive coupled translations only, as an example of experiments in which some parameters can be measured separately.

There are many complications that we have omitted in this paper. Among them are the full three dimensional formulation with anisotropic interface parameters which depend on all five characterizing angles, a non-linear S , shapes (interfaces that are not circular cylinders or flat planes) that require accommodations, elastic energies, effects of triple junctions in absorbing dislocations, etc. Because of the rotation in some of these processes, γ , as well as S and M , which are functions of θ are not constant. Their variation will surely affect the details of the kinetics. Stresses, whether applied or not, affect the processes. For non-circular grains stresses will be generated by these grain boundary processes and the kinetics will be modified by them. Some of these issues (including anisotropy in γ and more general cylindrical shapes) are dealt with in the companion paper [5]; others await future work.

Note added in proof

In Eq. (18) we used only the change in F resulting from the conversion of a volume of grain B to grain A , and ignored any possible dependence of $f_V (= f_V^B - f_V^A)$ on changes in the misorientation θ . Since only B rotates for the shrinking circular cylinder of Section 4, $\frac{df_V}{d\theta} = \frac{df_V^B}{d\theta}$, and

$$\frac{d}{dt}(\pi r^2 f_V) = 2\pi r f_V \frac{dr}{dt} + \pi r^2 \frac{\partial f_V^B}{\partial \theta} \frac{d\theta}{dt}.$$

If f_V^B depends on θ , the second term must be included in the effective stress term $(\sigma - \frac{\gamma'}{r})$ to give a combined effective stress term $(\sigma - \frac{\gamma'}{r} - \frac{1}{2} \frac{\partial f_V^B}{\partial \theta})$ in all equations of Section 4 in which this stress term appears, beginning with Eq. (18). An interesting anomaly arises in the limit as the radius r tends to infinity: This term does not drop out, reflecting the enormous volume it acts on. Eqs. (21) and (22) reduce to the planar case of Eqs. (2) and (3) only where $\frac{\partial f_V}{\partial \theta} = 0$.

Acknowledgement

We are grateful to S.G. Srinivasan of Los Alamos National Laboratory, who stimulated our interest and has been generous in making many of his old unpublished simulations results available to us.

References

- [1] Sutton AP, Balluffi RW. *Interfaces in Crystalline Materials*. Oxford: Clarendon Press; 1995 (Chapter 9, pp. 522 and Section 12.8.1, pp. 745).
- [2] Love AEH. *A Treatise on the Mathematical Theory of Elasticity*. fourth ed. New York: Dover; 1944. p. 33.
- [3] Christian JW. *The theory of transformations in metals and alloys*. second ed.. Oxford: Pergamon; 1975.
- [4] Srinivasan SG, Cahn JW. In: Ankem S, et al., editors. *Science and technology of interfaces*. Seattle: TMS; 2002. p. 3–14.
- [5] Taylor JE, Cahn JW. Grain rotation with coupling and surface diffusion, preprint.
- [6] Li C-H, Edwards EH, Washburn J, Parker ER. *Acta Metall* 1953;1:223.
- [7] Haslam AJ, Moldovan D, Yamakov V, Wolf D, Phillpot SR, Gleiter H. *Acta Mater* 2003;51:2097.
- [8] Harris KE, Singh VV, King AH. *Acta Mater* 1998;46:2623.
- [9] Upmanyu M, Smith RW, Srolovitz DJ. *Interface Sci* 1998;6:41.
- [10] Moldovan D, Wolf D, Phillpot SR. *Acta Mater* 2001;49:3521.
- [11] Warren JA, Kobayashi R, Lobkovsky AE, Carter WC. *Acta Mater* 2004;51:11.
- [12] Hermann G, Gleiter H, Baro G. *Acta Metall* 1976;24:353.
- [13] Chan S-W, Balluffi RW. *Acta Metall* 1985;33:1113; Chan S-W, Balluffi RW. *Acta Metall* 1986;34:2191.
- [14] Cahn JW. In: Handwerker CA, Blendell JE, Kaiser WA, editors. *Sintering of advanced ceramics*. American Ceramic Society; 1990; *Ceramic Trans* 1989;7:185.
- [15] Martin G. *Phys Stat Solidi B* 1992;172(1):121.
- [16] Srinivasan SG. Unpublished results.
- [17] Mullins WW. *Acta Met* 1956;4:421.
- [18] Molodov DA, Gottstein G, Heringhaus F, Shvindlerman LS. *Acta Mater* 1998;46:5627.
- [19] Deus AM, Fortes MA, Ferreira PJ, Vander Sande JB. *Acta Mater* 2002;50:3317.
- [20] Mura T. *Micromechanics of defects in solids*. second ed. Boston: Kluwer; 1987.
- [21] Friedel G. *Bull Soc Fr Mineral* 1933;56:262.
- [22] Koch E. *International tables for crystallography*, vol. C. Boston: Kluwer; 1992. Section 1.3.
- [23] Mott NF. *Proc Phys Soc* 1948;60:391.
- [24] Read WT, Shockley W. *Phys Rev* 1950;78:275.
- [25] Hanson D, Wheeler MA. *J Inst Metals* 1931;45:229.
- [26] Hanson D. *Trans AIME* 1939;133:15.